Vacancy-Assisted Diffusion of Alkoxy Species on Rutile TiO_2(110)

Zhenrong Zhang,[1] Roger Rousseau,[1,*] Jinlong Gong,[2] Shao-Chun Li,[3] Bruce D. Kay,[1] Qingfeng Ge,[4] and Zdenek Dohnálek[1,+]

[1]*Pacific Northwest National Laboratory, Fundamental and Computational Sciences Directorate and Institute for Interfacial Catalysis, Richland, Washington 99352, USA*

[2]*Department of Chemical Engineering, Center for Materials Chemistry, University of Texas at Austin, Texas 78712, USA*

[3]*Department of Chemistry and Biochemistry, Center for Materials Chemistry, University of Texas at Austin, Texas 78712, USA*

[4]*Department of Chemistry and Biochemistry, Southern Illinois University, Carbondale, Illinois 62901, USA*

(Received 30 April 2008; published 8 October 2008)

Using scanning tunneling microscopy (STM) and density functional theory simulations, we have studied the diffusion of alkoxy species formed by the dissociation of alcohols on bridge-bonded oxygen (BBO) vacancies (BBO_V's) on TiO_2(110). At elevated temperatures ($\geq$400 K) the sequential isothermal STM images show that mobile BBO_V's mediate the diffusion of alkoxy species by providing space for alkyl-group-bearing BBO atom to diffuse into. The experimental findings are further supported by simulations that find that BBO_V diffusion is the rate limiting step in the overall diffusion mechanism.

DOI: 10.1103/PhysRevLett.101.156103 PACS numbers: 68.47.Gh, 68.37.Ef, 73.43.Cd, 82.65.+r

The catalytic and photocatalytic properties of TiO_2 have attracted widespread interest in a variety of applications, such as air purification, self-cleaning glass, water splitting, solar cells, and wastewater treatment [1,2]. In many cases the catalytic chemistry of reducible oxides is dominated by oxygen vacancy sites. For reduced rutile TiO_2(110)-1 $\times$ 1, the bridge-bonded oxygen (BBO) vacancies (BBO_V's) are the most prevalent surface defects [3–5] which have been shown to readily dissociate small molecules such as H_2O, O_2, and alcohols [6–15].

Despite the fact that surface diffusion is an important process in heterogeneous catalytic reactions, very little is known about the mobility of adsorbates and reaction intermediates on TiO_2(110). To date, only the diffusion of water and hydrogen formed as a result of water dissociation on BBO_V's, have been extensively studied [8–11]. Recently our studies of alcohols on TiO_2(110) have shown their dissociation via O-H bond scission on BBO_V's to form paired alkoxy and hydroxyl species [7,12]. Here we demonstrate for the first time that BBO_V's can also catalyze the transport of adsorbed species. Specifically, we show that at elevated temperatures ($\geq$400 K), 2-butoxy diffusion does not occur via C-O bond cleavage and alkyl group motion. Instead, mobile BBO_V's assist diffusion of 2-butoxy groups by providing space for the alkyl-group-bearing BBO atom to diffuse into.

Experiments were performed in an ultrahigh vacuum chamber (base pressure $<8 \times 10^{-11}$ Torr) equipped with variable-temperature scanning tunneling microscopy (STM, Omicron). The TiO_2(110) (Princeton Scientific) was cleaned by cycles of Ne^+ sputtering and vacuum annealing to 900–950 K. 2-butanol (Sigma-Aldrich, 99.5%), methanol (Fisher, 99.9%), and 1-octanol (Sigma-Aldrich, 99 + %) were purified by several freeze-pump-thaw cycles using liquid nitrogen and introduced at room temperature onto the TiO_2(110) surface in the STM stage via a retractable tube doser. The sample temperature in the STM was controlled by a tungsten filament heater located behind the sample. The temperature reading was postcalibrated using a thermocouple (type K, Chromel-Alumel) attached directly to the sample surface. The estimated uncertainty in the temperature measurement is $\pm$15 K. A more detailed description of the experimental setup and procedures has been presented in our prior publications [3,9].

Calculations were carried out employing density functional theory (DFT) with a gradient corrected functional for exchange and correlation [16] as implemented in the CP2K package [17,18]. Core electrons are modeled as norm-conserving pseudopotentials and the wave functions expanded in a double-zeta Gaussian basis set with a plane wave auxiliary basis of 300 Ry energy cutoff, and the Γ point for Brilluoin zone integration. Calculation of all reaction coordinates was performed using the climbing-image nudged-elastic-band method (CI NEB) [19–21] employing seven beads. The coordinate for each reaction in our mechanism, as obtained from NEB, were verified by normal mode analysis of the transition state to determine that it represented a saddle point on the potential energy surface. All surface reactions are modeled on a (4 $\times$ 2) rutile-TiO_2(110) surface slab of 4 TiO_2 units depth and an ethoxy as a representative alkoxy group.

To address the effect of the excess electron from partially reduced Ti atoms created in the formation of BBO_V's on alkoxy diffusion we compared all mechanisms using both standard gradient corrected functionals [16] and the local density approximation plus on-site repulsion U (LDA + U) method [21] with the same exchange correlation functional and U = 5.5 eV as previously determined based on valence bond Hamiltonian embedded cluster

models [22]. The localization of the excess electrons achieved by employing the LDA + U method yielded identical results to those obtained with standard DFT to within 0.2 eV. Hence, our simulations suggest that the mechanism is not dependent upon the nature of the excess electrons.

The diffusion of a 2-butoxy group is illustrated in the sequence of four isothermal STM images obtained at 400 K and displayed in Figs. 1(a)–1(d) (for a complete sequence see the STM movie [23]). The corresponding ball models underneath illustrate the mechanism of the diffusion. In the empty state STM images, the low lying Ti^{4+} ions are imaged as protrusions while the rows of BBO ions are imaged as depressions due to the inverse electronic contrast of these two ions. In general, upon adsorption, the alcohol molecules dissociate on BBO_V's via O-H bond cleavage creating alkoxy/hydroxyl pairs with alkoxy healing the original BBO_V and hydroxyl occupying the neighboring BBO [11–15]. Based on our prior STM study [12], features identified after 2-butanol adsorption are the 2-butoxys that appear brightest (Fig. 1, red arrow), hydroxyls that are medium bright (Fig. 1, yellow arrow), and BBO_V's that are the least bright (Fig. 1, green arrows). In these images both BBO_V's [3] and hydroxyls [9] diffuse exclusively along the BBO rows with fairly high hopping rates, 4.8×10^{-3} s^{-1} and 3.0×10^{-3} s^{-1}, respectively, and are practically at the limit of motions that can be tracked using our slow scanning speeds (~1 min/image) while the 2-butoxy species are barely moving (5.0×10^{-5} s^{-1}).

In the following discussion we focus on the changes observed in the small area highlighted with rectangles in Figs. 1(a)–1(d). In this particular area the 2-butoxy stayed motionless for 35 min (not shown) prior to the acquisition of the image shown in Fig. 1(a) while the hydroxyls and BBO_V's readily diffused around. The 2-dimensional (2D) line scan [Fig. 1(a), cyan dashed line] along the BBO row in Fig. 1(e), clearly illustrates the large differences in the apparent height of the 2-butoxy and BBO_V species. After two minutes [Fig. 1(b)], the upper BBO_V moved along the BBO row towards the 2-butoxy. In the 2D line scan [Fig. 1(e), red] it is recognizable only as a small shoulder on the right side of the 2-butoxy feature. After an additional minute [Fig. 1(c)] the 2-butoxy and BBO_V features combined and formed a broad bright feature with a full width at a half maximum (FWHM) ~15% larger than that of the isolated 2-butoxy species. Further, this feature is centered between the two BBO positions as shown in 2D profile in Fig. 1(e), blue trace. After an additional six minutes [Figs. 1(d) and 1(e), green] the broad feature splits back into 2-butoxy and BBO_V. The BBO_V feature is now on the opposite side of 2-butoxy and the 2-butoxy feature is displaced by one lattice unit.

To acquire meaningful statistics, we have evaluated ~100 events between 400–415 K, the temperature range where both the 2-butoxy and BBO_V motion can be followed in our experiments. In all cases, the observed 2-butoxy diffusion events involved the BBO_V as well as the broad intermediate feature. This clearly indicates that BBO_V's mediate the 2-butoxy diffusion in this temperature range. As discussed below, DFT calculations show that the broad feature is due to the 2-butoxy—BBO_V pair rapidly switching positions and therefore in our experiments represents the time average of 2-butoxy moving between the two neighboring lattice positions. As expected, the formation of the broad intermediate feature led to the 2-butoxy

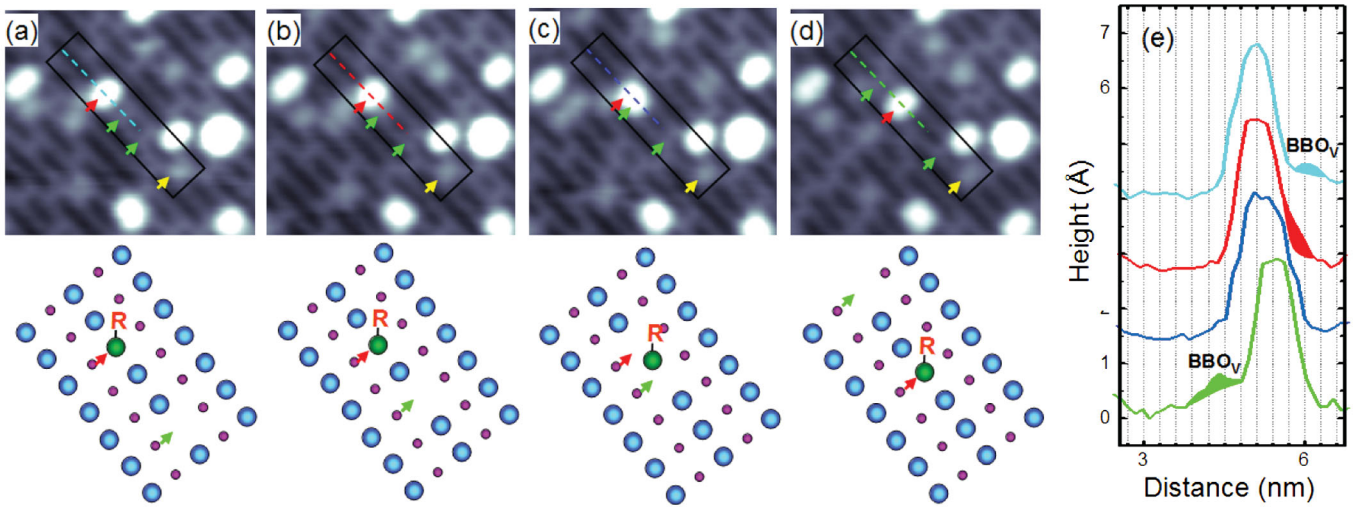

FIG. 1 (color). (a)–(d) Sequential STM images recorded at 400 K on the same area of 2-butanol preadsorbed TiO_2 (110) as a function of time (t = 0, 2, 3, 9 min). The rectangles mark the area of interest and contain one 2-butoxy (red arrow), two BBO_V's (green arrows), and one hydroxyl (yellow arrow) species. The corresponding ball models (BBO: blue, Ti^{4+}: magenta, and alcohol oxygen: green) illustrate the diffusion process. (e) 2-dimensional line profiles along the BBO row marked with the dashed lines in images (a)–(d). The vertical dashed lines in (e) mark the lattice positions along the BBO row.

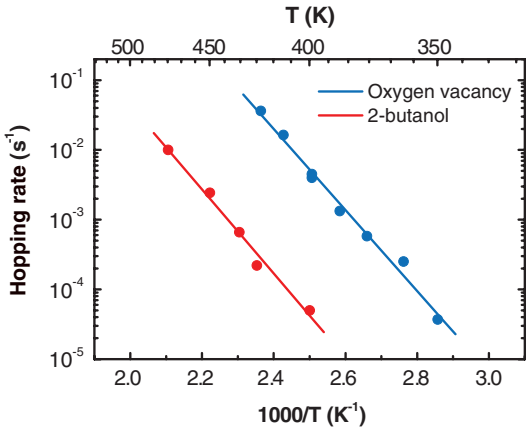

FIG. 2 (color). Arrhenius plots of the BBO_V [3] and 2-butoxy hopping rates along the BBO rows on TiO_2(110). Symbols represent the experimentally determined hopping rates with their statistical error bars being within the symbol size. Lines are fits to the Arrhenius equation. The diffusion barrier and preexponential factors determined from the fits are 1.15 ± 0.05 eV and $10^{12.2\pm0.6}$ s^{-1} for BBO_V's and 1.18 ± 0.05 eV and $10^{10.3\pm0.9}$ s^{-1} for 2-butoxy species.

diffusion only in ~50% of the cases. In the remaining ~50%, where BBO_V's did not switch position with 2-butoxys, the 2-butoxy features remained in their original position. Control experiments show that the tip does not perturb any of the observed diffusion measurements.

To determine the value of the diffusion barrier for 2-butoxy species, we carried out the isothermal experiments analogous to that shown in Fig. 1 at different temperatures and extracted the temperature-dependent hopping rates. At higher temperatures, as the hopping rate increases, it becomes increasingly likely that a certain fraction of 2-butoxy hops are undetected (e.g., back and forth motion). To account for this we use a mathematical analysis for a 1-dimensional random walk [3,24]. The extracted temperature-dependent 2-butoxy hopping rates, h, are displayed as an Arrhenius plot in Fig. 2 (red). The best fit to Arrhenius equation, $h = \nu \exp(-E_b/k_BT)$, yields values of the prefactor, ν, and the diffusion barrier, E_b. For comparison, the BBO_V hopping rates on clean TiO_2(110) determined in our previous study [3] are also shown (blue). The 2-butoxy and BBO_V data yield diffusion barriers of 1.18 ± 0.05 and 1.15 ± 0.05 eV, respectively. The fact that the values are statistically identical suggests that the BBO_V diffusion towards the 2-butoxy is the rate limiting step determining the overall diffusion barrier of the 2-butoxy species. Further, the fact that the prefactor, $\nu = 10^{10.3\pm0.9}$ s^{-1}, for the 2-butoxy diffusion is 2 orders of magnitude smaller than that for BBO_V's ($10^{12.2\pm0.6}$ s^{-1}) [3] also supports the BBO_V mediated mechanism. In the statistically simplest case, where the probability of finding the vacancy at any distance from the 2-butoxy species is identical, the value of BBO_V prefactor should be reduced by the BBO_V coverage (~0.10 ML) and the probability of having the BBO_V reflect back without the 2-butoxy diffusion (0.5). These factors reduce the BBO_V prefactor to $1 \times 10^{10.9\pm0.6}$ s^{-1}, which is within the experimental error of the value determined for the 2-butoxy diffusion.

In order to check whether the BBO_V assisted diffusion mechanism is applicable to other alkoxy species, we have also carried out a subset of the experiments using methanol and 1-octanol. The involvement of BBO_V's in the diffusion process as well as the presence of the broad bright intermediate feature was clearly observed for the case of methoxy diffusion. Since the 1-octoxy feature is much larger than the BBO_V, the intermediate feature could not be resolved, but the involvement of the BBO_V's was clearly observed. The diffusion kinetic parameters were determined only for 1-octoxy species. The diffusion barrier of 1.10 ± 0.03 eV is very close to that for BBO_V diffusion and the prefactor is ~3 orders of magnitude smaller than that for BBO_V diffusion. These measurements suggest that BBO_V assisted diffusion mechanism is also applicable to other alkoxy species.

To further understand the mechanism of alkoxy diffusion, we have employed periodic DFT simulations [16] and examined the potential energy surface for alkoxy species on TiO_2(110). The simplest, diffusion mechanism, involving C-O bond cleavage and motion of the alkyl group between the two BBO atoms, is shown in Fig. 3(a). The calculated barrier for this process is 2.0 eV which is significantly larger than the value of 1.18 eV determined experimentally.

The elementary steps calculated for the BBO_V assisted alkoxy diffusion mechanism are shown in Fig. 3(b). The initial step is diffusion of a BBO_V towards the alkoxy with the calculated barrier of 1.3 eV in agreement with 1.15 eV for BBO_V diffusion on clean TiO_2(110) [3]. We find that the value of this barrier varies only slightly (~0.1 eV) with the BBO_V—alkoxy distance. Note, the BBO_V diffusion is, in fact, diffusion of a neighboring BBO atom in the opposite direction. Similarly, the case of BBO_V assisted alkoxy diffusion is accomplished by diffusion of the alkyl-group-bearing BBO atom. Despite this similarity, the barrier calculated for motion of the alkyl-group-bearing BBO is 0.6 eV, which is less than half that for the bare BBO atom, and results from the oxygen of the alkoxy having a formal charge of −1, as opposed to −2 for BBO's, which sub-

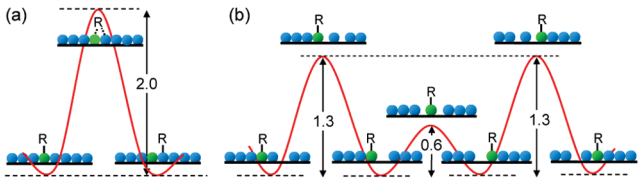

FIG. 3 (color). Calculated diffusion paths for two possible diffusion mechanisms: (a) alkyl group diffusion between the two BBO atoms (blue balls) on a BBO row. (b) BBO_V assisted diffusion of alkoxy group.

stantially reduces the electrostatic attraction with the Ti cations. This low diffusion barrier value explains the presence of the broad bright intermediate feature observed in our STM experiments [Fig. 1(e), blue]. Using the theoretically determined barrier difference and assuming the same prefactor for the BBO_V and 2-butoxy hops we estimate that at 400 K the neighboring 2-butoxy and BBO_V switch positions $\sim 1.4 \times 10^8$ times before the BBO_V diffuses away. Further we can determine the BBO_V hopping rate away from the 2-butoxy experimentally using the average lifetime of the broad bright intermediate feature. At 400 K, we obtain a value of 190 s which corresponds to a BBO_V hopping rate of 5.2×10^{-3} s^{-1}. This hopping rate is similar to the BBO_V's hopping rate on bare $TiO_2(110)$ [3] suggesting that the BBO_V diffusion is not significantly affected by the presence of neighboring 2-butoxy species. In agreement with the interpretation of our experimental results, the DFT calculations also show that the BBO_V diffusion is the rate limiting step in the diffusion of 2-butoxy species.

In summary, we present experimental measurements and first principles simulations of BBO_V assisted adsorbate diffusion on $TiO_2(110)$. The sequences of isothermal high resolution STM images directly show that the diffusion of alkoxy groups along the BBO rows is assisted by BBO_V's. Arrhenius analysis yields a 2-butoxy diffusion barrier of 1.18 eV, close to 1.15 eV determined for BBO_V diffusion [3]. This suggests that BBO_V diffusion is the rate limiting step in 2-butoxy diffusion. The DFT and DFT + U calculations are in very good agreement with experiment and combined suggest that a negligible role is being played by the excess electrons associated with the BBO_V. This work, apart from presenting a novel diffusion mechanism for adsorbates on oxide surfaces, also raises questions about the role of BBO_V's in mass transport on these catalytically important surfaces.

We thank N. A. Deskins, M. Dupuis, M. A. Henderson, and N. Govind for useful discussion. This work was supported by the U.S. Department of Energy Office of Basic Energy Sciences, Chemical and Material Sciences Division, Robert A. Welch Foundation (F-0032), and National Science Foundation (CHE-0412609). J. G. would like to acknowledge the support from PNNL through Summer Research Institute. The experimental work as well as the theoretical calculations were performed at W. R. Wiley Environmental Molecular Science Laboratory (EMSL), a national scientific user facility sponsored by the Department of Energy's Office of Biological and Environmental Research located at Pacific Northwest National Laboratory (PNNL). PNNL is operated for the U.S. DOE by Battelle under Contract No. DEAC0676RLO 1830. Computational resources were provided by the Molecular Science Computing Facility (EMSL) and the National Energy Research Scientific Computing Center at Lawrence Berkeley National Laboratory.

*Corresponding author.
Roger.Rousseau@pnl.gov
†Corresponding author.
Zdenek.Dohnalek@pnl.gov

[1] T. L. Thompson, and J. T. Yates, Top. Catal. **35**, 197 (2005).
[2] H. J. Freund, H. Kuhlenbeck, and V. Staemmler, Rep. Prog. Phys. **59**, 283 (1996).
[3] Z. Zhang *et al.*, Phys. Rev. Lett. **99**, 126105 (2007).
[4] U. Diebold, Surf. Sci. Rep. **48**, 53 (2003).
[5] C. Di Valentin, G. Pacchioni, and A. Selloni, Phys. Rev. Lett. **97**, 166803 (2006).
[6] O. Bikondoa *et al.*, Nature Mater. **5**, 189 (2006).
[7] Z. Zhang *et al.*, J. Am. Chem. Soc. **128**, 4198 (2006).
[8] S. Wendt *et al.*, Phys. Rev. Lett. **96**, 066107 (2006).
[9] S. C. Li *et al.*, J. Am. Chem. Soc. **130**, 9080 (2008).
[10] N. G. Petrik and G. A. Kimmel, Phys. Rev. Lett. **99**, 196103 (2007).
[11] Z. Zhang *et al.*, J. Phys. Chem. B **110**, 21840 (2006).
[12] Z. Zhang *et al.*, J. Phys. Chem. C **111**, 3021 (2007).
[13] L. Gamble, L. S. Jung, and C. T. Campbell, Surf. Sci. **348**, 1 (1996).
[14] M. A. Henderson, S. Otero-Tapia, and M. E. Castro, Faraday Discuss. **114**, 313 (1999).
[15] O. Bondarchuk *et al.*, J. Phys. Chem. C **111**, 11059 (2007).
[16] J. P. Perdew, K. Burke, and M. Ernzerhof, Phys. Rev. Lett. **77**, 3865 (1996).
[17] J. Vande Vondele *et al.*, Comput. Phys. Commun. **167**, 103 (2005).
[18] G. Lippert, J. Hutter, and M. Parrinello, Mol. Phys. **92**, 477 (1997).
[19] G. Henkelman, B. P. Uberuaga, and H. Jonsson, J. Chem. Phys. **113**, 9901 (2000).
[20] G. Mills, H. Jonsson, and G. K. Schenter, Surf. Sci. **324**, 305 (1995).
[21] V. I. Anisimov, J. Zaanen, and O. K. Andersen, Phys. Rev. B **44**, 943 (1991).
[22] C. J. Calzado, N. C. Hernández, and J. F. Sanz, Phys. Rev. B **77**, 045118 (2008).
[23] See EPAPS Document No. E-PRLTAO-101-030842 for an atomically resolved movie of vacancy assisted 2-butoxy diffusion on $TiO_2(110)$ at 400 K. For more information on EPAPS, see http://www.aip.org/pubservs/epaps.html.
[24] J. D. Wrigley, M. E. Twigg, and G. Ehrlich, J. Chem. Phys. **93**, 2885 (1990).